Open- and Closed-Loop Analysis of the 70-Meter Antenna Subreflector Positioner

F. Baher[1]

The subreflector of the 70-m antenna moves in threes axes—the x-, y-, and z-directions—and rotates about the z-axis. The subreflector controller performs the motion control of these movements. In order to maintain antenna pointing accuracy, the subreflector must focus the radio frequency beam that moves with the structural deformations as the antenna rotates in azimuth and elevation. This article presents analysis and development of the control system model of the subreflector positioner, describes the control system specifications, and presents the control system performance, such as overshoot, settling time, bandwidth, and phase and gain margins.

I. Introduction

Due to defocusing of the radio frequency beam that arises from gravity-induced structural deformations as the antenna rotates about the elevation axis, the subreflector must be continuously moved to compensate for the antenna deformation. The movement is supervised by the subreflector controller (SRC). The subreflector controller assembly provides automatic offset correction in the axial (z)- and lateral (y)-axes. This is accomplished by two independently adjusted motion mechanisms comprising electric motors and a jackscrew. The x-displacement and rotation axes do not require offset correction. The lateral (y)- and axial (z)-displacements require offset correction with respect to the antenna elevation angle. The offset corrections are downloaded from the subreflector controller computer and stored in the memory of the programmable logic controller (PLC) in the subreflector drive cabinet (SRDC). The distance the subreflector travels in in the y- and z-axes is calculated by equations that represent the theoretical position as compared with the actual position on the subreflector with respect to the antenna elevation angle.

To accomplish this, the subreflector controller receives a position command from the uplink computer at a rate of 50 Hz. The commanded position is routed to the SRDC to process the subreflector motion. The controller in the SRDC calculates the current position of each axis with transducers providing the position data, which the controller requires for calculations. The current position from the SRC is compared with the desired position. The difference, the error, is fed to the proportional controller to actuate the drive that moves the subreflector to a new position.

---

[1] Communications Ground Systems Section.

The research described in this publication was carried out by the Jet Propulsion Laboratory, California Institute of Technology, under a contract with the National Aeronautics and Space Administration.

This article discusses the subreflector positioner controller and the performance of its open- and closed-loop system. The article also provides the development of the Simulink model for the subreflector positioner.

II. Subreflector Positioner Assembly

The subreflector moves in three axes—the x-, y-, and z-axes—and rotates around the z-axis. The positioner assembly and the orientations of all axes are shown in Fig. 1 while the maximum travel range for each axis is given in Table 1. There are a total of six actuators (x; y1 and y2; and z1, z2, and z3) that provide the subreflector positioner with six degrees of freedom. Each one of the six identical axis drives consists of a motor, a gearbox, jackscrew spindle, and a transducer. The rotation axis also consists of a dual-drive anti-backlash system.

The antenna pointing assembly (APA) initiates a command signal to track and point the antenna to the target. This is accomplished by transmitting the elevation angle from the angle encoders of the antenna servo control assembly at a rate of 20 Hz. It is received by the communication board of the SRC via an RS232 interface. The current positions of the axes are received from the SRDC via local area network (LAN) interface.

When the antenna operates in signal-receiving mode, the incoming parallel rays of RF energy strike the primary reflective parabola, more or less uniformly illuminating the entire surface. This incoming signal is then reflected from the primary dish surface onto the hyperbolic surface of the subreflector. The subreflector, in turn, reflects the energy from the primary reflector into the secondary focal point, which can be any one of three microwave subsystem feed cones located on the cone assembly.

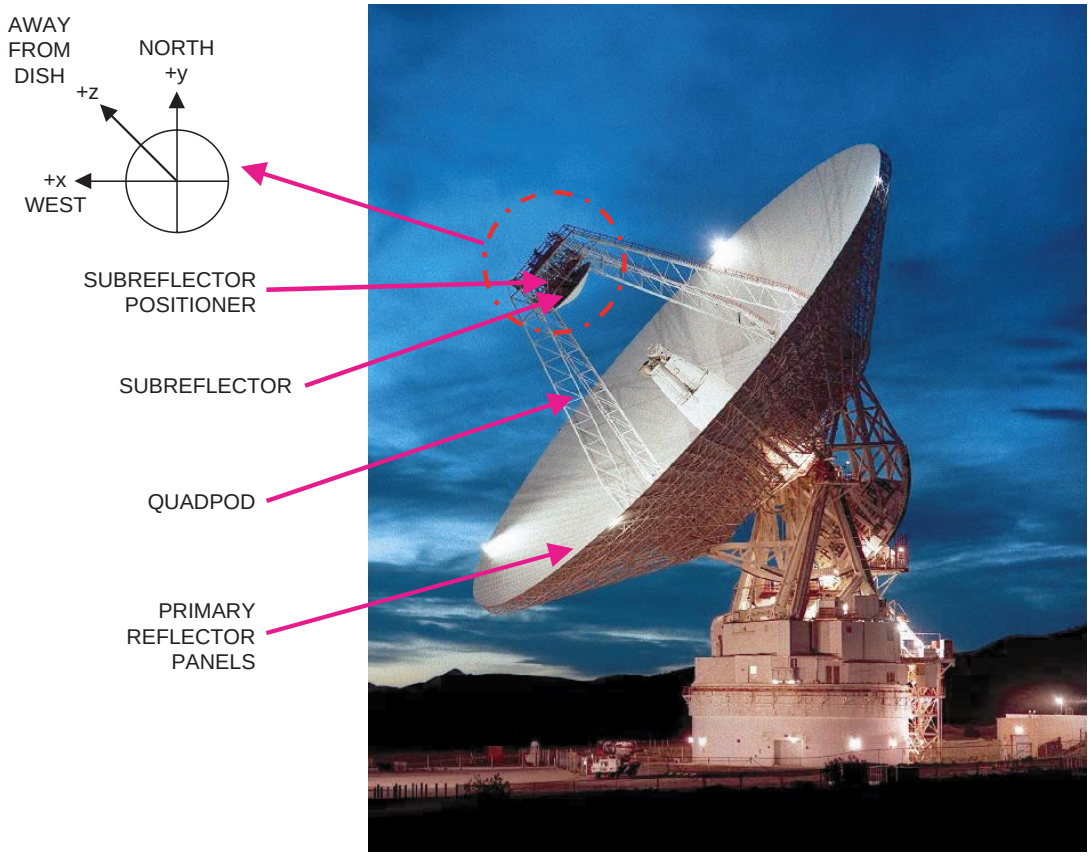

Fig. 1. The 70-m antenna subreflector positioner assembly.

Table 1. Subreflector positioner parameters and specifications.

Parameter	Specification
Subreflector diameter	8 m
Torus diameter	2.04 m
Mass of subreflector	6,300 kg
Mass of torus structure	4,300 kg
Mass moment of inertia for each x- and y-direction	20,000 kg-m^2
Mass moment of inertia for each z-direction	50,400 kg-m^2
Mass of spindle, motor, gearbox, clutch, and universal joint	280 kg
Mass of subreflector and torus gravity	106 kN
For 3 jacks in the z-axis	88 N
For 2 jacks in the y-axis	131 N
For 1 jack in the x-axis	265 N
Mass of subreflector and torus (ice)	24.9 kN
Beam stiffness	150×10^{-6} N/m
Axis travel acceleration	0.025 m/s^2
Subreflector linear travel speed	0.00127 m/s (3 in./min)
Rotational speed	0 deg/s to 4 deg/s
Rotational acceleration (minimum)	1 deg/s^2
Linear position accuracy	0.00005 m (0.002 in.)
Rotation accuracy	0.0022 deg
Axis travel limits	
For the x-axis	±0.0762 m (±3 in.)
For the y-axis	+0.127 m (+5 in.) to −0.1778 m (−7 in.)
For the z-axis	+0.10668 m (+4.2 in.) to −0.1143 m (−4.5 in.)

Selection of the feed focal points is accomplished by the SRC issuing a position command to move the subreflector either clockwise or counterclockwise depending on the shortest route to reach the new feed focal position. This position command is then routed through the SRDC and then passed on to the subreflector junction boxes, where the subreflector motor starter receives it as an input. The subreflector rotation motors will then drive the subreflector until the selected focal point position has been reached. Further optimization of the RF beam alignment with respect to any one of the feed focal points is possible by automatically adjusting the subreflector position linearly along lateral (y)- and axial (z)-axes.

As shown in Fig. 2,[2] the SRC receives antenna elevation angle data from the antenna servo controller (ASC) to reposition the subreflector. The SRC processes the angle data, transmits the applicable commands to drive the actuators, and also receives position data from the SRDC via the SRC interface.

The operation of the drive motors and rate and position loops is controlled by the SRDC, which compares a table-generated position (the offset table of positions of the subreflector is a function of antenna elevation angle) of the subreflector in the x-, y-, and z-axes with the actual position as sensed by the position encoders, producing a position-error offset. If the error is greater than 0.00127 m, the SRDC determines the direction the motors must run to move the subreflector to the correct position, and then

[2] *70 m Antenna Subreflector Positioner—Overview and Mechanical*, DSN OMM-03612 (internal document), Jet Propulsion Laboratory, Pasadena, California, January 15, 1996.

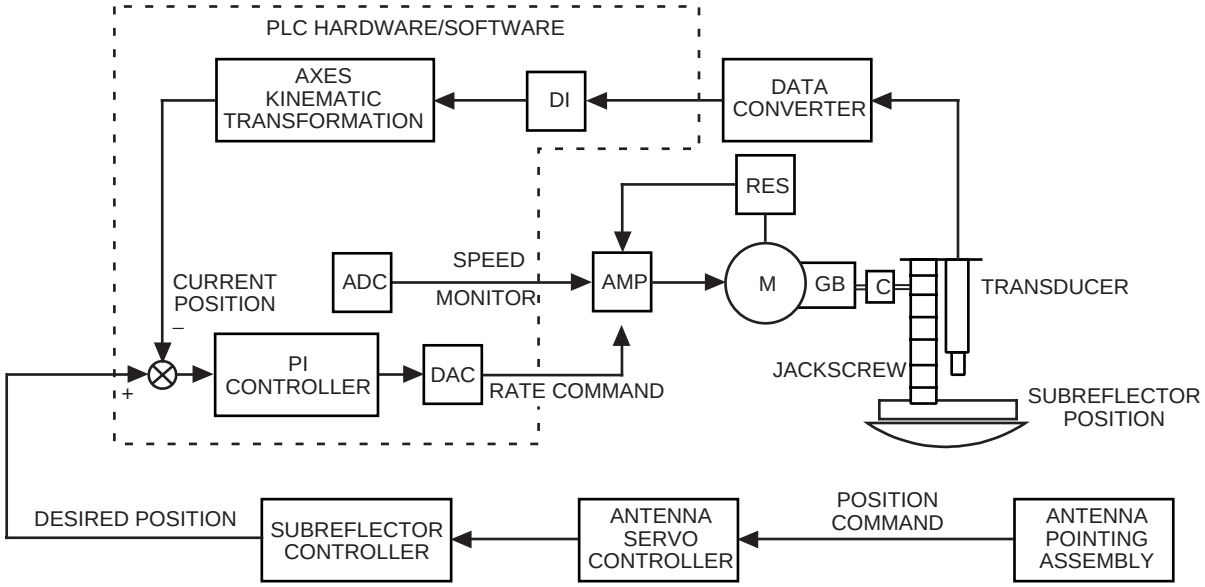

Fig. 2. A simplified block diagram of the subreflector positioner control system (DI = digital input, C = coupling, GB = gearbox, M = motor, RES = resolver, AMP = amplifier, ADC = analog-to-digital converter, DAC = digital-to-analog converter, PI = proportional integral)

transmits commands via the SRC LAN interface to the subreflector-positioner-mounted motor controller for that axis. The SRC controller generates subreflector subsystem status concerning the operation of the subreflector positioner assembly. The status is then sent to the uplink computer, which is accessible by the operations personnel.

III. Mechanical System Modeling

The mechanical system shown in Fig. 3 consists of combined rotational (motor and coupling) and translational (jackscrew and subreflector) subsystems. The translational force acting on the subreflector positioner is equal to the sum inertia forces due to the mass of the subreflector, torus, and universal joint and the force due to the stiffness of the universal joint. In this model, the subreflector is attached to the torus, and the torus is connected to the universal joint, which in turn is connected to the jackscrew. The jackscrew is supported by the motor, gear assemblies, and the second universal joint to the antenna structure.

A. Motor

The motors used in the subreflector positioner drives are Kollmorgens (model number B-204-B-39-5-062). They are brushless and low-inertia-type motors, which allows for rapid acceleration and deceleration. The resolver is an integral part of the drive motor. Subreflector positioner parameters and motor parameters are listed in Tables 1 and 2, respectively.[3]

B. Gearbox

The subreflector gearbox, Alpha Gear Drives model SPF110-M2-16, with a gear ratio of 16:1 is attached to the motor shaft, which in turn is connected to the jackscrew actuator to further reduce the motor motion and to control the subreflector. The physical parameters for the gearbox, mass moments of inertia, torsional rigidity, and gearbox ratio are given in Table 3. The shaft viscous damping and torsional backlash are assumed to be negligible.

[3] *70 m Antenna Subreflector Positioner Control System*, DSN OMM-03613 (internal document), Jet Propulsion Laboratory, Pasadena, California, January 15, 1996.

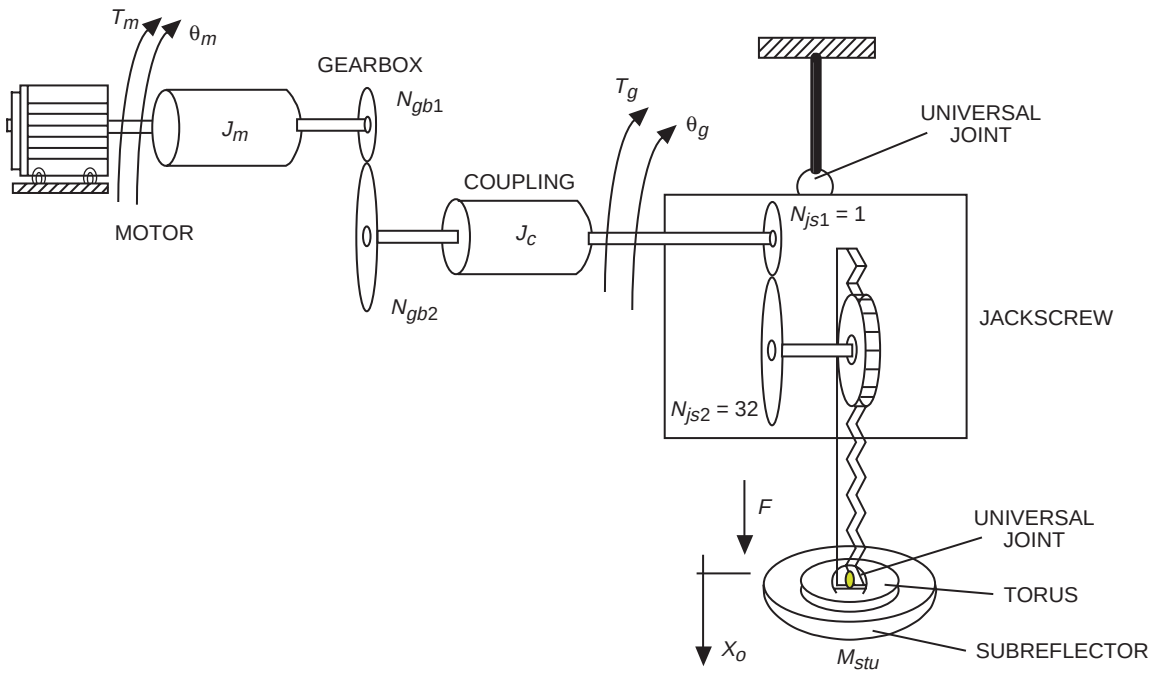

Fig. 3. The mechanical mode of the subreflector positioner drive system.

Table 2. Motor parameters.

Specification description	Symbol	Value	Unit of measure
Continuous power	Wp	0.81	kW
Maximum operating speed	W_{no}	3600	r/min
Maximum speed	Wl	1800	r/min
Continuous torque (Tstall)	T_c	4.47	N-m
Peak torque	Tp	10.0	N-m
	Tp	13.8	N-m
Motor resistance	R_a	2.48	ohms
Motor inductance	L_a	38.0	mh
Motor inertia	J_m	0.0001729	kg-m^2
Static friction	T_f	0.1	N-m
Viscous damping	F_i	8.5×10^{-5}	N-m-s/rad
Motor constant	K_m	0.464	N-m/$\sqrt{w}$
Back emf constant	K_b	0.49	V rms-s/rad
Motor torque constant	K_t	0.85	N-m/A rms

Table 3. Gearbox, jackscrew, coupling, and universal point parameters.

Parameter	Unit of measure	Gearbox	Coupling	Jackscrew	Universal joint
Moment of inertia J_g, J_c, Jj	kg-m^2	0.00017	0.0046	0.01	
Torsional rigidity (stiffness) K_g, K_c, K_j, K_{uj}	N-m/rad	137,536	40,447	37,000	400×10^6
Gear ratio N_g, Nj		16:1		0.375 rev/mm 2667 rev/m	

C. Coupling

The coupling, manufactured by KTR Corporation (model Lamex EFD42), connects the gearbox and the jackscrew. The coupling is backlash free, made from high-resistance plastic lamina, torsionally rigid, and flexible in bending.

D. Jackscrew

The jackscrew (PFAFF model HSE 100L-KU/BA) is an actuator for the subreflector positioner linear drive; it is a recirculating ball with a backlash-free nut inside a worm-gear unit.

E. Transducer and Resolver

The actual positions and motions of the x-, y-, and z-axes are measured by linear position transducers in conjunction with a data converter, model MK292. The transducer is mounted in parallel to the jackscrew. One end of the linear transducer is fixed at the jackscrew and the other end is connected to the end flange of the jackscrew via a bearing unit with a rotational degree of freedom only. The rate-loop feedback is obtained from resolvers that are connected to drive motors and provides a scale factor of 8 V per 3600 r/min.

IV. Electronics

A. Amplifier

The motor drive amplifier, a Kollmorgen industrial drive (model number BDS4A-206J-204B21P), is used to drive the motor. The performance parameters of the amplifier are shown in Table 4.[4] Since the dynamics of the amplifier are much faster than the response of the motor, the amplifier is modeled as a DC gain.

B. Hardware

The heart of the subreflector positioner servo drive system is the Siemens Programmable Logic Controller (PLC). The PLC provides capability and flexibility to meet all control-system requirements, such as high-speed processing time, rate loop, controller, computation of complex math, and communication interface with the host computer SRC. The main task of the PLC is to perform servo drive functions and motion interlock, to position the spindle legs, to position the drives and anti-backlash drive unit, to close the rate and position loops, to calculate the overall position x-, y-, and z-axes and rotation, and to communicate with the subreflector controller.

[4] Ibid.

Table 4. Amplifier parameters.

Characteristic	Performance standard
Input command rate	±10 VDC differential
Resolver feedback signal	±8 V/3600 r/min
Gain	0.45
Bandwidth	30 Hz

C. Software

The Labview and Matlab support software tools were used to facilitate data measurement and system analysis.

V. Subreflector Positioner Rate and Position-Loop Modeling

The subreflector positioner assembly and position control system are designed to meet the requirements and specifications stated in Table 1.[5] The schematic of the physical system is provided in Fig. 4. From the schematic, the state–space model can be obtained using physical laws of Newton for motion and Kirchhoff for electrical circuits. Next, the Simulink and Matlab control tool is used (discrete-time system) to create open- and closed-loop models and to simulate the subreflector performance.

Figure 5 shows the Simulink rate-loop model while Fig. 6 illustrates the subreflector position-loop model. The model is entirely parameter-based except for the unit conversion factors. All numerical values are programmed in the Matlab file "param.m." This method provides the flexibility to modify parameters for the model in the file without altering the Simulink model.

A. Mechanical Subsystem Model

The torque of the motor is the sum of inertia, damping, and the torque at the output of the gearbox (see Fig. 4),

$$T_m = J_e\ddot{\theta}_m + D\dot{\theta}_m + \frac{1}{N_g}T_g \tag{1}$$

and the gearbox torque is defined as

$$T_g = K_e(\theta_g - \theta_c) \tag{2}$$

Substituting for T_g in Eq. (1), one obtains

$$J_e\ddot{\theta}_m + D_m\dot{\theta}_m + \frac{K_e(\theta_g - \theta_c)}{N_g} = T_m \tag{3}$$

The armature current and the torque are related as follows:

[5] *70-m Antenna Subreflector Positioner Technical Requirement Document*, TRD 515962 (internal document), Jet Propulsion Laboratory, Pasadena, California, March 15, 1993.

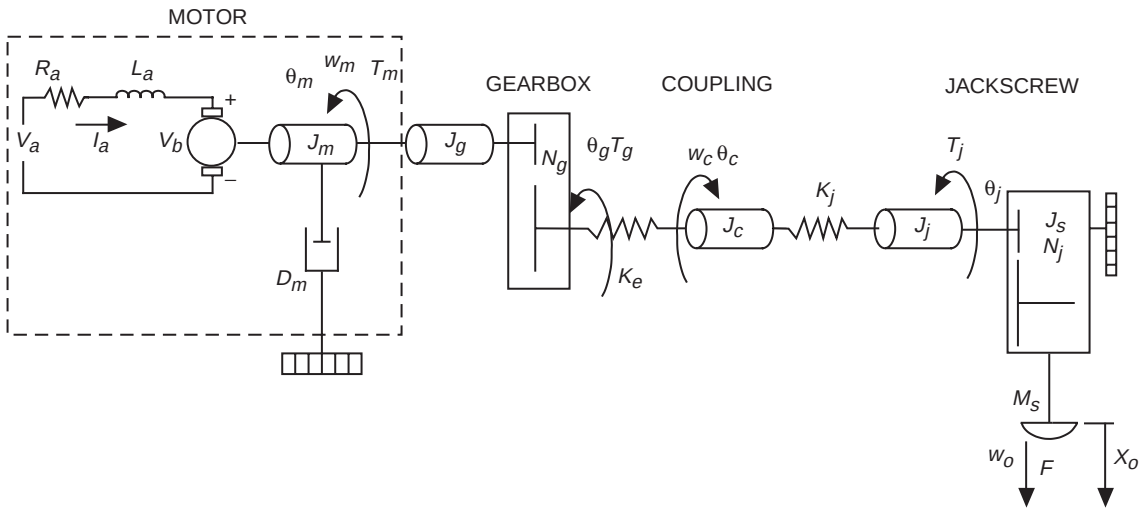

Fig. 4. The subreflector model.

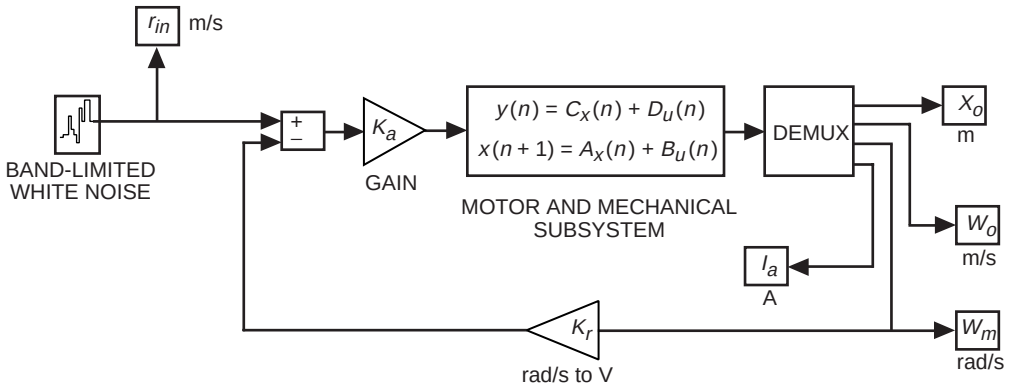

Fig. 5. The Simulink model of the rate-loop system.

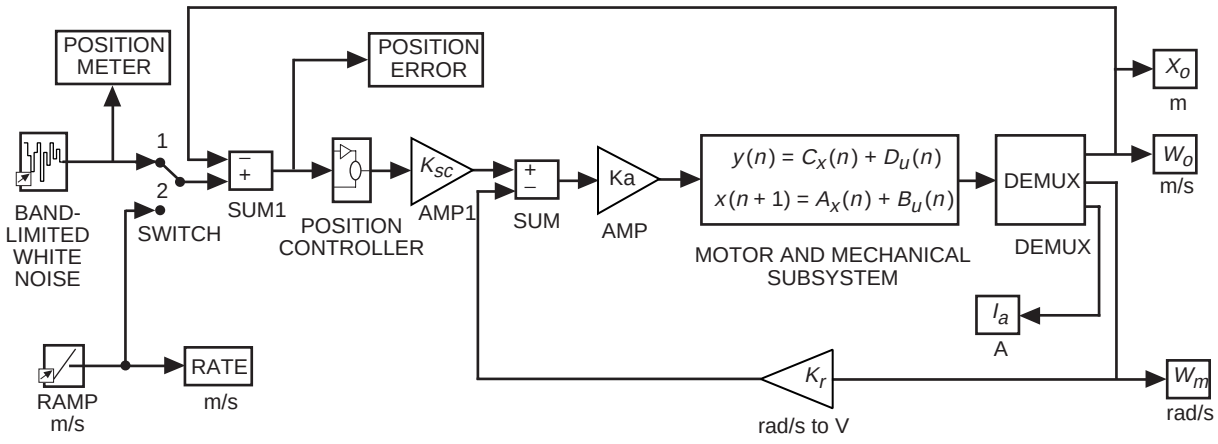

Fig. 6. The Simulink model of the closed-loop system.

$$T_m = K_t I_a \tag{4}$$

The remaining parameters of Eq. (3) are as follows:

$$\left.\begin{aligned} J_e &= J_m + J_g \\ K_e &= \frac{K_g K_c}{K_g + K_c} \\ \theta_g &= \frac{\theta_m}{N_g} \end{aligned}\right\} \tag{5}$$

and T_m is the motor torque, and J_e, D_m, and K_e are the equivalent inertia, damping, and stiffness, respectively, reflected at the jackscrew. The rotational displacements at the output of the motor shaft gearbox are θ_m and θ_g, respectively.

Substituting for θ_g in the above equation, one obtains

$$J_e\ddot{\theta}_m + D_m\dot{\theta}_m + \frac{K_e}{N_g^2}\theta_m - \frac{K_e}{N_g}\theta_c = T_m = K_t I_a \tag{6}$$

The torques at the coupling follow from Fig. 4:

$$J_c\ddot{\theta}_c + K_e(\theta_c - \theta_g) + K_j(\theta_c - \theta_j) = 0 \tag{7}$$

The rotational displacement of the jackscrew, θ_j, is proportional to the translational displacement of the subreflector, X_o, by

$$X_o = \frac{\theta_j}{N_j} \tag{8a}$$

or

$$\theta_j = N_j X_o \tag{8b}$$

Substituting for θ_j in Eq. (7), one obtains

$$J_c\ddot{\theta}_c - \frac{K_e}{N_g}\theta_m + (K_e + K_j)\theta_c - N_j K_j X_0 = 0 \tag{9}$$

From Fig. 6, the torques at the jackscrew can be written as

$$J_j\ddot{\theta}_j + K_j(\theta_j - \theta_c) + T_j = 0 \tag{10}$$

The jackscrew torque, T_j, is a result of angular acceleration and is equal to the product of the force acting on the subreflector and inversely proportional to the jackscrew gear ratio, N_j:

$$T_j = \frac{F}{N_j} \tag{11}$$

The force acting on the subreflector positioner is

$$F = M\ddot{X}_o \tag{12}$$

where $\ddot{X}_o$ is the acceleration of the subreflector.

Substituting Eq. (12) into Eq. (11), the governing equation for the jackscrew model is

$$T_j = \frac{F}{N_j} = \frac{M_s}{N_j}\ddot{X}_o \tag{13}$$

Substituting Eqs. (12) and (13) into Eq. (10) and simplifying, one obtains

$$J_j\ddot{\theta}_j + K_j(\theta_j - \theta_c) + \frac{M_s}{N_j}\ddot{X}_o = 0 \tag{14}$$

or

$$(N_j^2 J_j + M_s)\ddot{X}_o + N_j^2 K_j X_o - N_j K_j \theta_c) = 0 \tag{15}$$

The motor armature voltage is

$$V_a = R_a I_a + K_b\omega_m + L_a i_a \tag{16}$$

The equations of motion of the subreflector positioner are summarized as follows:

$$\ddot{\theta}_m = -\frac{D_m}{J_e}\omega_m - \frac{K_e}{N_g^2 J_e}\theta_m + \frac{K_e}{N_g J_e}\theta_c + \frac{K_t}{J_e}I_a \tag{17}$$

$$\ddot{\theta}_c = \frac{K_e}{N_g J_c}\theta_m - \frac{K_e + K_j}{J_c}\theta_c + \frac{K_j N_j}{J_c}x_o \tag{18}$$

$$\ddot{x}_o = \frac{N_j K_j}{N_j^2 J_j + M_s}\theta_c - \frac{N_j^2 K_j}{N_j^2 J_j + M_s}x_o \tag{19}$$

$$i_a = -\frac{R_a}{L_a}I_a - \frac{K_b}{L_a}\omega_m + \frac{1}{L_a}V_a \tag{20}$$

In matrix form, Eqs. (17) through (20) can be written as

$$\dot{X} = AX + BU \tag{21}$$

$$Y = CX \tag{22}$$

where X is a 7×1 state vector, U is the input voltage to excite the motor, Y is the output vector, A is a 7×7 square state matrix, B is a 7×1 input matrix, and C is a 4×7 output matrix. The state vector is defined as

$$X = \begin{bmatrix} \theta_m \\ \omega_m \\ \theta_c \\ \omega_c \\ x_o \\ \omega_o \\ I_a \end{bmatrix} \tag{23a}$$

and the outputs are the subreflector position, x_o; velocity, ω_o; motor velocity, ω_m; and current, I_a, in the given axis,

$$Y = \begin{bmatrix} \omega_m & x_o & \omega_o & I_a \end{bmatrix} \tag{23b}$$

where

$$A = \begin{bmatrix} 0 & 1 & 0 & 0 & 0 & 0 & 0 \\ -\dfrac{K_e}{N_g^2 J_e} & -\dfrac{D_m}{J_e} & \dfrac{K_e}{N_g J_e} & 0 & 0 & 0 & \dfrac{K_t}{J_e} \\ 0 & 0 & 0 & 1 & 0 & 0 & 0 \\ \dfrac{K_e}{N_g J_c} & 0 & -\dfrac{(K_e + K_j)}{J_c} & 0 & \dfrac{N_j K_j}{J_c} & 0 & 0 \\ 0 & 0 & 0 & 0 & 0 & 1 & 0 \\ 0 & 0 & \dfrac{N_j K_j}{N_j^2 J_j + M_s} & 0 & -\dfrac{N_j^2 K_j}{N_j^2 J_j + M_s} & 0 & 0 \\ 0 & -\dfrac{K_b}{L_a} & 0 & 0 & 0 & 0 & -\dfrac{R_a}{L_a} \end{bmatrix} \tag{24}$$

$$B = \begin{bmatrix} 0 \\ 0 \\ 0 \\ 0 \\ 0 \\ 0 \\ \dfrac{1}{L_a} \end{bmatrix} \tag{25a}$$

and

$$C = \begin{bmatrix} 0 & 0 & 0 & 0 & 1 & 0 & 0 \\ 0 & 0 & 0 & 0 & 0 & 1 & 0 \\ 0 & 1 & 0 & 0 & 0 & 0 & 0 \\ 0 & 0 & 0 & 0 & 0 & 0 & 1 \end{bmatrix} \tag{25b}$$

B. Rate-Loop Model

The subreflector rate-loop model shown in Fig. 5 includes the motor, amplifier, and mechanical components. The current loop is closed in the servo amplifier. The transfer function, obtained by injecting a white noise signal with a sampling time of 0.002 s, is applied as a rate command to the summing junction, and the output is taken at the resolver feedback. As shown in the model, the scaling factor in the feedback path is for conversion from the rate command (rad/s) to volts in order to match the voltage from the resolver.

The open-loop transfer function is shown in Fig. 7. As the plot shows, the rate loop at a −3 dB roll-off has a bandwidth of about 38 Hz and a phase of −62 deg. The gain is about −1 dB. As is seen from the plot, a slight resonance is visible at approximately 11.5 Hz.

The difference between the two simulation plots may contribute to uncertainties in some parameter values. Many parameter variations, such as stiffness, mass, and inertia, were simulated to see their effects on the oscillations, which occurred at about 11.5 Hz, showing that only motor inertia has a significant effect on the resonance peak. The dashed line shows the frequency response under nominal conditions, while the solid line represents an increase by 2 in inertia and assumes the motor inductance impedance is negligible as compare with the armature resistance.

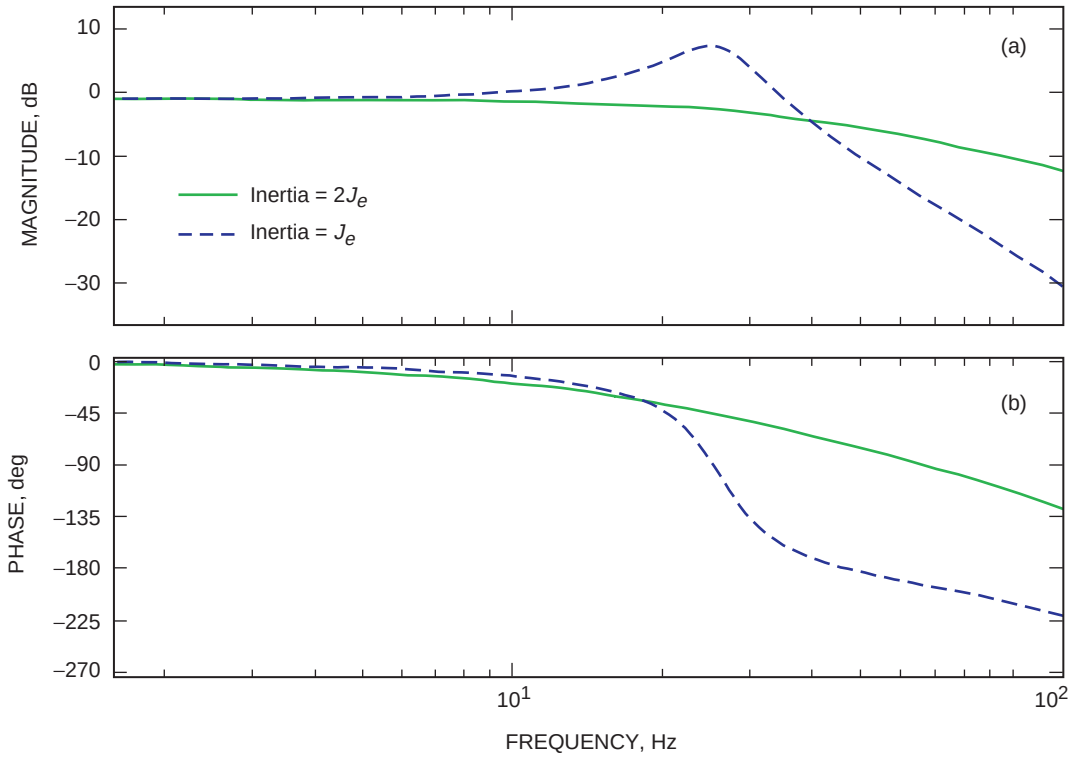

Fig. 7. Simulated subreflector rate-loop frequency response: (a) magnitude and (b) phase.

The open-loop frequency response measurements (resolver) were performed with the use of a Hewlett Packard (HP) 3562A frequency analyzer and the step response tests, using a strip chart recorder. From the HP analyzer, a sweep sine signal of 0.5 V peak to peak was injected into the amplifier terminal block (the connector between the digital-to-analog (D/A) converter module and the amplifier was removed, and the HP analyzer input signal was connected in its place) as a velocity command, and the output was taken from the resolver feedback (the D/A PLC module).

Frequency response measurements were obtained from 0.1 to 100 Hz, and gain and phase were averaged for two measurements for each set of data taken. Several tests were made while the antenna was moving up/down and at elevation angles of 45 and 88 deg and an azimuth angle of 180 deg. However, the results for all the tests were the same, and Fig. 8 shows the frequency response at 45-deg elevation. The gain of the rate loop is about −7 dB with a bandwidth of 28 Hz and phase of about 57 deg.

Figure 9 shows two plots of simulated and experimental step responses. Figures 9(a) shows rate-loop response to a step input. As is shown from the plot, the velocity peaks at about 100 r/min and approaches zero when the subreflector reaches the desired position. The settling time is about 2 s with no overshoot. In Fig. 9(b), a position command of 0.000254 m was initiated, and the output response was measured at the tachometer feedback. As is shown in the figure, for a small step input, the tachometer voltage peaks at about 1.3 V and approaches zero as the subreflector reaches the final position. The settling time is approximately 2 s, which is the same as the simulated one.

C. Position-Loop Model

The Simulink block diagram for the position closed-loop system is shown in Fig. 6. The switch is set to position 1 to simulate a position command. The discrete model with a sampling time of 0.02 s is chosen to model the actual discrete-time controller. The frequency response of the system position from

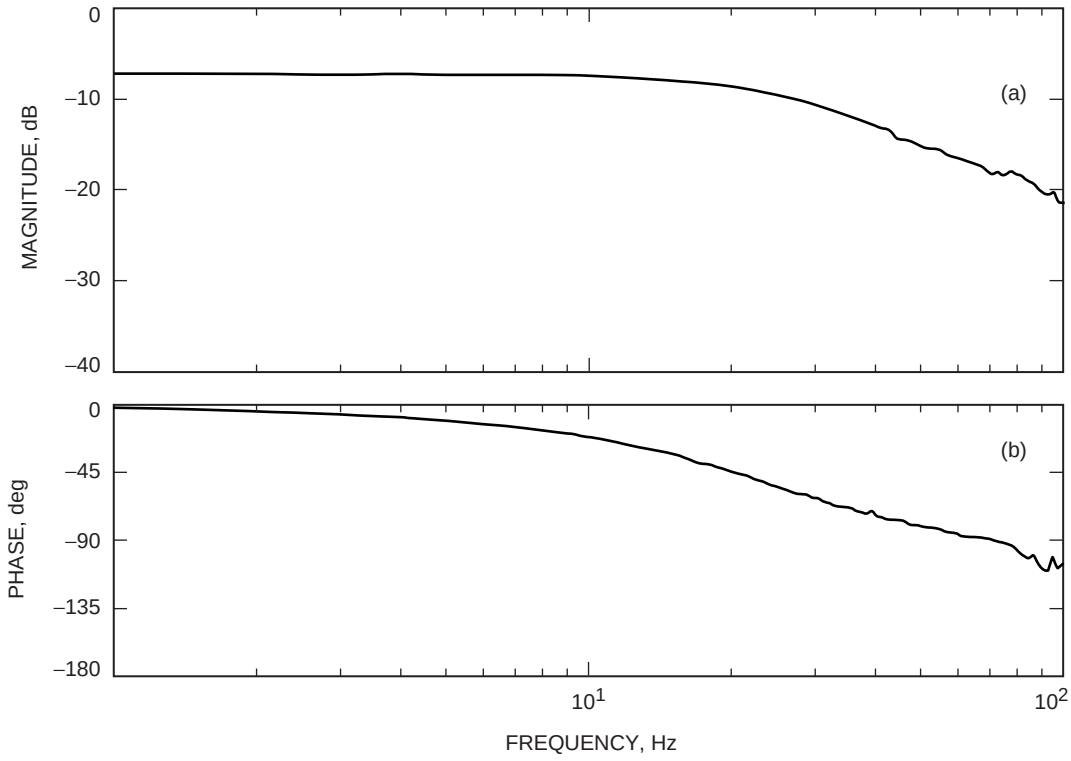

Fig. 8. Frequency response of the subreflector rate-loop system: (a) magnitude and (b) phase.

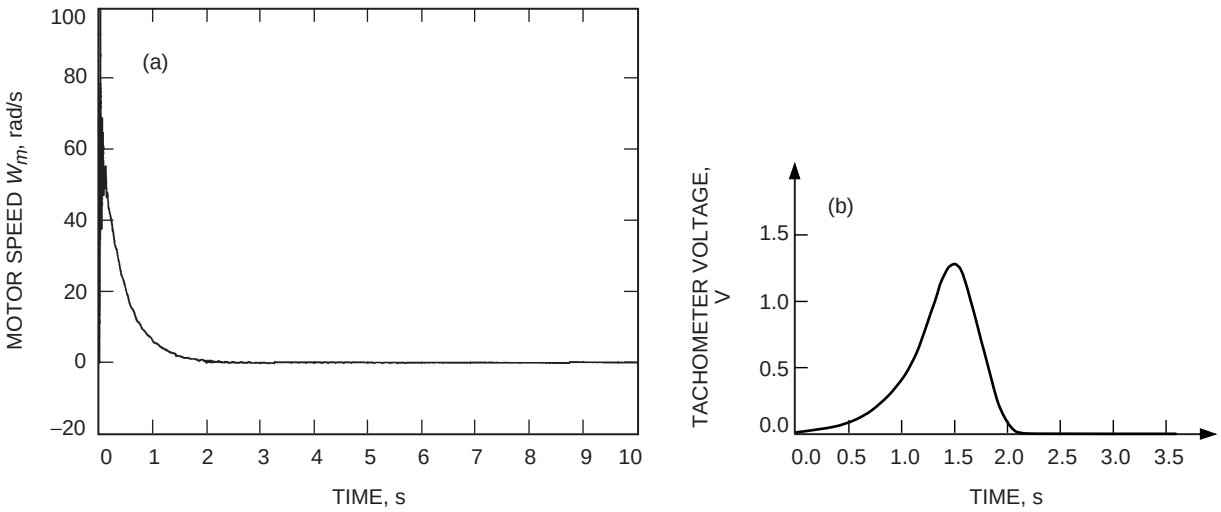

Fig. 9. The subreflector rate-loop response to the step input: (a) simulated and (b) measured.

the position command to the transducer position is simulated. In the actual system, the position loop is closed in the PLC, and the transducer gain is compensated in the analog-to-digital (A/D) converter in the PLC assembly. In the simulation model, the unity feedback and scaling factor in the forward loop are used to model the equivalent position feedback.

The controller for the subreflector position loop is a simple proportional controller with a gain of $K_p = 10$. The simulated closed-loop model has a gain of 1 (0 dB) with a bandwidth of approximately 0.5 Hz.

As shown in Fig. 10, a slight resonance is visible at approximately 11.5 Hz. The dashed line represents the nominal inertia of the simulated closed-loop response, and the solid one shows that the oscillation is removed by increasing the motor and gearbox by 2 times. However, this resonance is way beyond the −3 dB roll-off and will not affect the subreflector performance.

Figure 11 shows the response of the subreflector closed loop when a small step input of 0.0001 m is applied. From the plot, it can be seen that the settling time is approximately 2 s. The settling time of the closed-loop system was measured by commanding the subreflector to move to incremental positions of 0.0000254 m, 0.000254 m, and 0.00254 m and was recorded in slightly less than 2 s, which compared well and agreed with the value obtained from the simulation.

VI. Conclusions

In this article, the models of the closed- and open-loops of the subreflector positioner were developed. The models provide parameters of the subreflector positioner such as structural inertia, stiffness, and the actuator data. The equations of motion were developed, and the step and frequency responses for parameter variations were provided.

The simulation results show that the results of the mathematical analysis for the rate and position loops correspond to the existing mechanical parameters. The closed-loop dynamic parameters of overshoot, settling time, and bandwidth were verified.

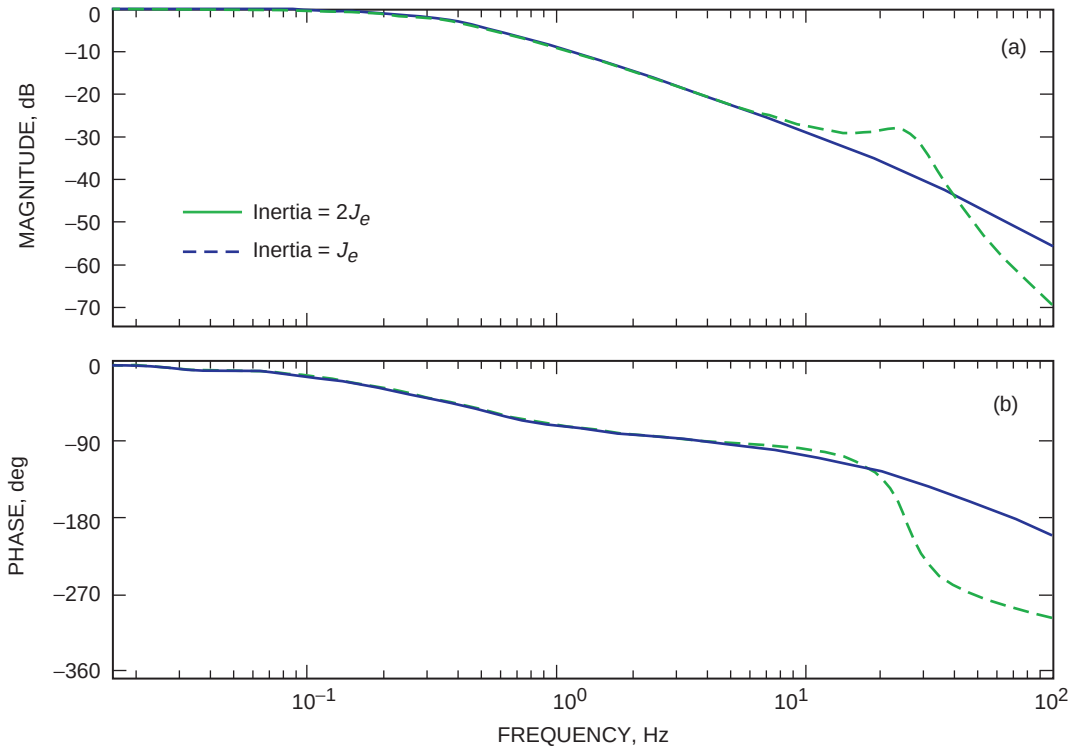

Fig. 10. The subreflector closed-loop frequency response: (a) magnitude and (b) phase.

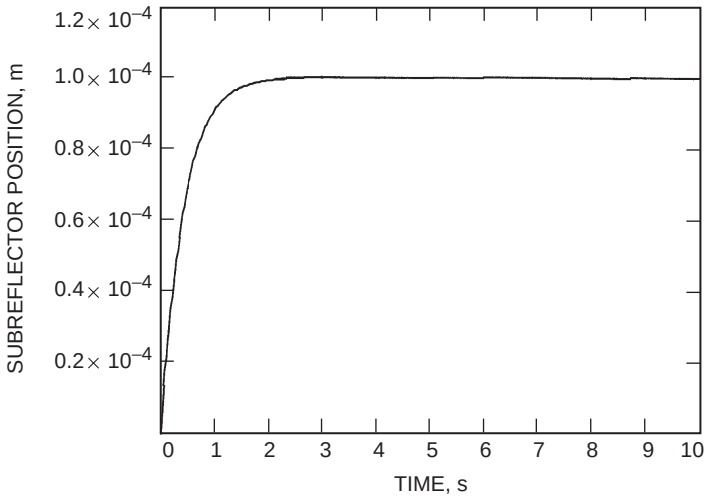

Fig. 11. The response of the subreflector closed-loop system to the step-input command.

Acknowledgments

The author would like to acknowledge support of this work by Scott Morgan. My special thanks to Wodek Gawronski for his technical support and review of this article. I would like to thank Robert Haroldsson, who facilitated and helped to make the measurements possible.